Electronic Supporting Information

Synergistic non-bonding interactions based on diketopyrrolopyrrole for elevated photoacoustic imaging-guided photothermal therapy †

Fang Liu,[a b] Feiyan Ma,[a] Qing Chen,[a] Enbao Zhou,[a] Puwen Zhang, [c] Zhanjun Cui, [*a] Zhonghua Liu, and Yongwei Huang, [*a]

a. Laboratory for NanoMedical Photonics, School of Basic Medical Science, Henan University, Kaifeng 475004 China. E-mail: E-mail: czj1968@126.com (Z. Cui) and huanyw@henu.edu.cn (Y. Huang)

b. The First Affiliated Hospital of Henan University, Kaifeng 475004, P.R. China.

c. School of Pharmacy, Henan University, Kaifeng 475004, P. R. China.

1. Materials and methods

All reagents were purchased from commercial sources and used without further purification unless otherwise noted. ^{1}H NMR spectra were measured with a Bruker Avance 400 MHz spectrometers by using $CDCl_3$ as the solvent. UV-Vis adsorption spectra were recorded on Perkin-Elmer Lamda 950 UV-Vis spectroscopy. Fluorescence spectra were recorded by using a Perkin-Elmer LS 55 luminescence spectrometer. TEM measurement was acquired using a TECHNAI G2 20 S-TWIN transmission electron microscopy (200 KV). The TEM sample was prepared by directly dropping nanoparticle dispersion (20 μg mL^{-1}) onto a carbon film and dried on a warm table at 30 °C. Dynamic light scattering (DLS) was performed on a Malvern ZETASIZER Nano ZS90 system.

The theoretical calculation was performed using density functional theory (DFT) provided by the DMol3 code. [1-3] The Perdew and Wang parameterization of the local exchange correlation energy are applied in the local spin density approximation (LSDA) to describe exchange and correlation.[4] We expanded the all-electron spin-unrestricted Kohn-Sham wave functions in a local atomic orbital basis. In such double-numerical basis set polarization was described. All calculations were all-electron ones, and performed with the Extra-Fine mesh. Self-consistent field procedure was done with a convergence criterion of 10^{-5} a.u. on the energy and electron density.

2. Synthesis of the DPP-SS, DPP-OF, DPP-SF, DPP-SeF.

Synthetic of DPP-SeF: 3,6-bis(5-bromoseleno-2-yl)-2,5-bis(2-octyldodecyl)pyrrolo [3,4-c]pyrrole-1,4(2H, 5H)-dione (114.9 mg) and 3,4-difluoroselenophene-2,5-diyl-bis(trimethylstannane) (44.5 mg) were put into a three-neck flask (50 mL), then addition 10 mL anhydrous toluene, and dissolved by ultrasound for 5 min. After rinsing with Argon gas for 20 min, add $Pd(PPh_3)_4$ (20 mg), then rinse with argon for 10 min to remove the gas as far as possible. In the temperature of 110 ℃ reaction for 24 h. After decompression removal the solvent, Soxhlet extraction to purified the product. After cooled to room temperature, methanol (100 mL) was used to precipitate the resultant, and then the precipitate filtered through Soxhlet extraction with methanol, n-hexane, and chloroform, respectively. After reduced pressure removal the solvent, the resulted polymer was further purified by

precipitation in methanol again, finally vacuum drying gives a dark blue solid (85 mg, 74.7%). ^{1}H NMR (400 MHz, $CDCl_3$): δ 9.16-8.75 (d, 2 H), 7.98-7.90 (m, 2 H), 7.50 (m, 1 H), 7.12 (s, 1 H), 4.70 (m, 2 H), 4.36(m, 2 H), 2.18 (m, 2 H), 1.31-1.04 (m, 64 H), 0.79 (m, 12 H). GPC (THF, polystyrene standard), Mn: 1.92 × 10^4 g mol^{-1}; Mw: 2.95× 10^4 g mol^{-1}, PDI: 1.58.

Synthetic of the (DPP-SS): 3,6-bis(5-bromofuran-2-yl)-2,5-bis(2-octyldodecyl)pyrrolo [3,4-c]pyrrole-1,4(2H, 5H)-dione (105.5 mg) and 2,5-bis(trimethylstannyl)thiophene (40.9 mg) were put into a three-neck flask (50 mL), then addition 10 mL anhydrous toluene, and dissolved by ultrasound for 5 min. After rinsing with Argon gas for 20 min, add $Pd(PPh_3)_4$ (20 mg), then rinse with argon for 10 min to remove the gas as far as possible. In the temperature of 110 ℃ reaction for 24 h. After decompression removal the solvent, Soxhlet extraction to purified the product. After cooled to room temperature, methanol (100 mL) was used to precipitate the resultant, and then the precipitate filtered through Soxhlet extraction with methanol, n-hexane, and chloroform, respectively. After reduced pressure removal the solvent, the resulted polymer was further purified by precipitation in methanol again, finally vacuum drying gives a dark blue solid (70 mg, 69.5%). ^{1}H NMR (400 MHz, $CDCl_3$): δ 9.16-8.75 (d, 2 H), 7.98-7.90 (m, 2 H), 7.50 (m, 1 H), 7.12(s, 1 H), 4.70 (m, 2 H), 4.36(m, 2 H), 2.18 (m, 2 H), 1.31-1.04 (m, 64 H), 0.79 (m, 12 H). GPC (THF, polystyrene standard), Mn: 1.55 × 10^4 g mol^{-1}; Mw: 2.13× 10^4 g mol^{-1}, PDI: 1.65.

Synthetic of DPP-OF: 3,6-bis(5-bromofuran-2-yl)-2,5-bis(2-octyldodecyl)pyrrolo [3,4-c]pyrrole-1,4(2H, 5H)-dione, (102.3 mg) and 3,4-difluorofuran-2,5-diyl-bis(trimethylstannane) (44.5 mg) were put into a three-neck flask (50 mL), then addition 10 mL anhydrous toluene, and dissolved by ultrasound for 5 min. After rinsing with Argon gas for 20 min, add $Pd(PPh_3)_4$ (20 mg), then rinse with argon for 10 min to remove the gas as far as possible. In the temperature of 110 ℃ reaction for 24 h. After decompression removal the solvent, Soxhlet extraction to purified the product. After cooled to room temperature, methanol (100 mL) was used to precipitate the resultant, and then the precipitate filtered through Soxhlet extraction with methanol, n-hexane, and chloroform, respectively. After

reduced pressure removal the solvent, the resulted polymer was further purified by precipitation in methanol again, finally vacuum drying gives a dark blue solid (73mg 72%). ^{1}H NMR (400 MHz, $CDCl_3$): δ 9.16-8.75 (d, 2 H), 7.98-7.90 (m, 2 H), 7.50 (m, 1 H), 7.12(s, 1 H), 4.70 (m, 2 H), 4.36(m, 2 H), 2.18 (m, 2 H), 1.31-1.04 (m, 64 H), 0.79 (m, 12 H). GPC (THF, polystyrene standard), Mn: 1.86 × 10^4 g mol^{-1}; Mw: 2.63× 10^4 g mol^{-1}, PDI: 1.74.

Synthetic of the DPP-SF: 3,6-bis(5-bromofuran-2-yl)-2,5-bis(2-octyldodecyl)pyrrolo [3,4-c]pyrrole-1,4(2H, 5H)-dione (105.5 mg) and 3,4-difluorothiophene-2,5-diyl-bis(trimethylstannane) (44.5 mg) were put into a three-neck flask (50 mL), then addition 10 mL anhydrous toluene, and dissolved by ultrasound for 5 min. After rinsing with Argon gas for 20 min, add $Pd(PPh_3)_4$ (20 mg), then rinse with argon for 10 min to remove the gas as far as possible. In the temperature of 110 ℃ reaction for 24 h. After decompression removal the solvent, Soxhlet extraction to purified the product. After cooled to room temperature, methanol (100 mL) was used to precipitate the resultant, and then the precipitate filtered through Soxhlet extraction with methanol, n-hexane, and chloroform, respectively. After reduced pressure removal the solvent, the resulted polymer was further purified by precipitation in methanol again, finally vacuum drying gives a dark blue solid (78 mg 74%). ^{1}H NMR (400 MHz, $CDCl_3$): δ 9.16-8.75 (d, 2 H), 7.98-7.90 (m, 2 H), 7.50 (m, 1 H), 7.12(s, 1 H), 4.70 (m, 2 H), 4.36(m, 2 H), 2.18 (m, 2 H), 1.31-1.04 (m, 64 H), 0.79 (m, 12 H). GPC (THF, polystyrene standard), Mn: 1.86 × 10^4 g mol^{-1}; Mw: 2.73× 10^4 g mol^{-1}, PDI: 1.84.

3. Preparation of DPP-SS, DPP-OF, DPP-SF, and DPP-SeF NPs.

Conjugated polymer (1 mg) and DSPE-$mPEG_{2000}$ (3 mg) was dissolved in THF (1 mL) and fully dissolved by sonication. Then, a THF solution (1 mL) containing conjugated polymer (0.5 mg mL^{-1}) and DSPE-$mPEG_{2000}$ (1.5 mg mL^{-1}) was used to prepare NPs by rapidly injecting the solution into distilled-deionized water (10 mL) under continuous stirring. After injecting, THF was evaporated at room temperature under stirring for 24 h. The aqueous solution was filtered by filter (0.22 μm), and washed under centrifugation at 5000 rpm for 5 min. The concentrations of NPs solution were

determined by UV-vis absorption according to their absorption coefficients. The NPs solution were concentrated to 2 mg mL^{-1} by freeze drying and stored at 4 °C.

4. *In vitro* photothermal properties of the DPP-SS, DPP-OF, DPP-SF, DPP-SeF NPs.

The DPP-SS, DPP-OF, DPP-SF, DPP-SeF NPs (0.5 mL) with different concentrations (5, 10, 20 40 μg mL^{-1}) exposed to laser irradiation at 808 nm (0.75 W cm^{-2}) for 5 min, and the temperature was recorded using a photothermal camera Ti480 in the 5 min with an accuracy of ±0.1 °C. And then draw the temperature change curve at every 30 s in the 5 min. the befor and after irridition UV-vis spectra of NPs solution was detected to characterization their photothermal stability. To futher examination the photothermal stability of NPs, NPs (10 μg mL^{-1}) solution was irradiated with an 808 nm NIR laser for 5 min, then cooling for 5 min. The heating and cooling were repeated six times, and every 30 s recorded temperature.

5. Photothermal conversion efficiencies of the DPP-SS, DPP-OF, DPP-SF and DPP-SeF NPs.

To calculate the photothermal conversion e□ciency (η), NPs aqueous solution (20 μg mL^{-1}) was irradiatded at 808 nm for 10 min, the temperature was monitored by photothermal camera every 30 s in the irradiation. After the laser exposure, the temperature was continuously monitored every 30 s for 10 min when finally cooling to room temperature. According to available literature reports, the photothermal conversion efficiencies were calculated as follows:

η was determined according to equation (a):

$$\eta = \frac{hS\Delta T_{max} - Q_{Dis}}{I\left(1 - 10^{-A808}\right)} \quad \text{(a)}$$

where η indicate the heat transfer coefficient, *h* and *S* is parameters related to solvent and container, *h* means heat transfer coefficient and *S* stand for surface area of the container. ΔTmax is the maximum temperature change of solvent. *I* stand the laser power used for irradiation, A808 means the absorbance of the nanoparticle aqueous solution at 808 nm. Q_{Dis} stands for the heat input due to light absorption

by the solvent and container, and the Q_{Dis} was evaluated as 14 mW independently using pure water. *hS* can be determined by measuring the rate of temperature decrease after removing the light source according to equation (b):

$$\tau_s = \frac{m_D - C_D}{hS} \quad \text{(b)}$$

Where, the m_D and c_D indicate the mass (1.0 g) and heat capacity (4.2 J g^{-1}) of the waser in the solvent. τ_s is the time constant for heat transfer of the system, which can be calculated according to equation (c):

$$t = -\tau_s \ln(\theta) = -\tau_s \ln \frac{T_t - T_{Surr}}{T_{Max} - T_{Surr}} \quad \text{(c)}$$

where θ is indicate the ratio of ΔT and ΔT_{Max}. t is the cooling time points when turn off the laser for 10 mins. T_t is the corresponding temperature of PNPs during the cooling stage. T_{Max} means the maximum of the PNPs aqueous solution. T_{surr} stand for the temperature of the surrounding environment. From a plot of time against temperature during the cooling period, τ_s is calculated.

6. *In vitro* cytotoxicity of the DPP-SeF by MTT assay.

Human lung adenocarcinoma cells (A549) and Human small cell lung cancer (H446) with good growth conditions were selected and planted in 96-well plates and seed 6000 cells per well. The cells were incubated in a cell incubator at 37 °C overnight. After the cells are attached, drug incubation is performed. The medium was aspirat first and washed twice with sterile PBS. Then add 100 μL of fresh medium and 10 μL NPs solution with different concentrations to each well, and then incubate for 4 h. After that, the experimental group was irradiated with 808 nm laser. After the laser treatment, the cells were further cultured for 12 h to make the injured cells fully apoptotic, and then the cell viability was detected by MTT. The cell viability was judged by the absorbance at 492 nm of each well. Three replicate wells were set for each group, and the average value was finally taken as the result, and the standard deviation was added to determine the feasibility of the result. Finally, half inhibitory

concentrations were calculated based on the cell growth inhibitory rates of different concentrations of PNPs. All the cells used are obtained from the cell culture center of Institute of Basic Medical Sciences, Chinese Academy of Medical Sciences (Beijing, China). The medium was modulate by DMEM with 10% FBS.

7. *In vitro* cytotoxicity of the DPP-SeF NPs by Cell Imaging.

A549 cells with good growth status were planted in 6-well plates (3×10^5 cells / well) and cultured at 37 ° C for 24 hours. Four wells were randomly selected as different experimental groups, namely PBS, Laser, NPs, and NPs + Laser. Add 20 μg mL^{-1} of DPP-SeF NPs to the nano-solution treatment group. The grouo of NPs+Laser was irradiated with a 808 nm laser (0.75 W cm^{-2}). After irradiation and incubation for 12 hours, the cells were stained with calcein-AM (1 μmol L^{-1}) and propidium iodide (PI, 2 μmol L^{-1}) for 15 min and observed by inverted fluorescence microscope. Green fluorescence is cells in normal status and red fluorescence is apoptotic cells.

8. Flow cytometry analysis of the DPP-SeF NPs.

A549 cells were planted in 6-well plates (5×10^5 cells / well). After the cells were completely adhered, four wells were selected as PBS, Laser, NPs and NPs + Laser. NPs + Laser was irradiated with laser for 5 min (0.75 W cm^{-2}). After the laser treatment, the cells were incubated for another 24 h, and then the cells were stained using the Annexin V-FITC / PI kit (Solarbio). After incubation, the proportion of live cells and dead cells was detected by flow cytometer and statistics were performed.

9. Mice tumor model

Animal care and handling procedures were approved by the Animal Management and Ethics Committee of Henan University. All animal care and experimental protocols complied with the Animal Management Rule of the Ministry of Health, People's Republic of China (Documentation no. 55, 2001) 16-18 g female BALB / c nude mice were purchased from Vital River Company (Beijing, China). A549 cells (4×10^6 cells) were administered by subcutaneous injection in the armpit to establish a tumor model in female nude mice.

The photoacoustic signals of the mice were observed and imaged by a MOST imaging system (inVision 128; iThera Medical, Germany). Inject NPs (100 μL, 2 mg mL^{-1}) into tumor-bearing mice through the tail vein, and then scan the photoacoustic signals of the mice in different bands, observe and record the signal intensity of tissues and organs over time. The final result analyzed and reconstructed through the model-based algorithm supplied within the View MSOT software suite (V3.6, iThera Medical).

A near-infrared imager (Ti 480-FLUKE) was used to observe the temperature change of the tumor site during photothermal treatment. Tail vein inject PBS or DPP-SeF NPs (100 μL, 2 mg mL^{-1}) to Tumor-bearing mice. According to the photoacoustic imaging results, the tumor site was irradiated with laser (0.75W cm^{-2}) after injected NPs 9 hours . The imager observed and recorded the temperature during the irradiation. Variety. Finally, the infrared images at time points of 0, 1, 2, 3, 4, and 5 min were selected as schematic diagrams.

10. Antitumor effect of DPP-SeF NPs *in vivo*

When the tumor volume reached 100 ± 10 mm^3, the mice were equally divided into 4 groups, 6 mice in each group, and treated differently with PBS, Laser, DPP-SeF NPs and DPP-SeF NPs + Laser (100 μL, 2 mg mL^{-1}), all treatments were injected via the tail vein. After the DPP-SeF NPs + Laser group was injected with DPP-SeF NPs for 9h, irradiated tumor site with laser for 5 min (0.75 W cm^{-2}). After photothermal treatment, the mouse weight and tumor volume were weighed every two days, and the relative tumor volume was normalized to its initial size. After the end of the treatment process, the mice in each group were dissected, and the important organ and tumor tissues were subjected to H & E staining to analyze the physiological status and tumor treatment effect of the mice in each group. In addition, blood was collected for blood biochemical analysis to verify the biological safety of DPP-SeF NPs.

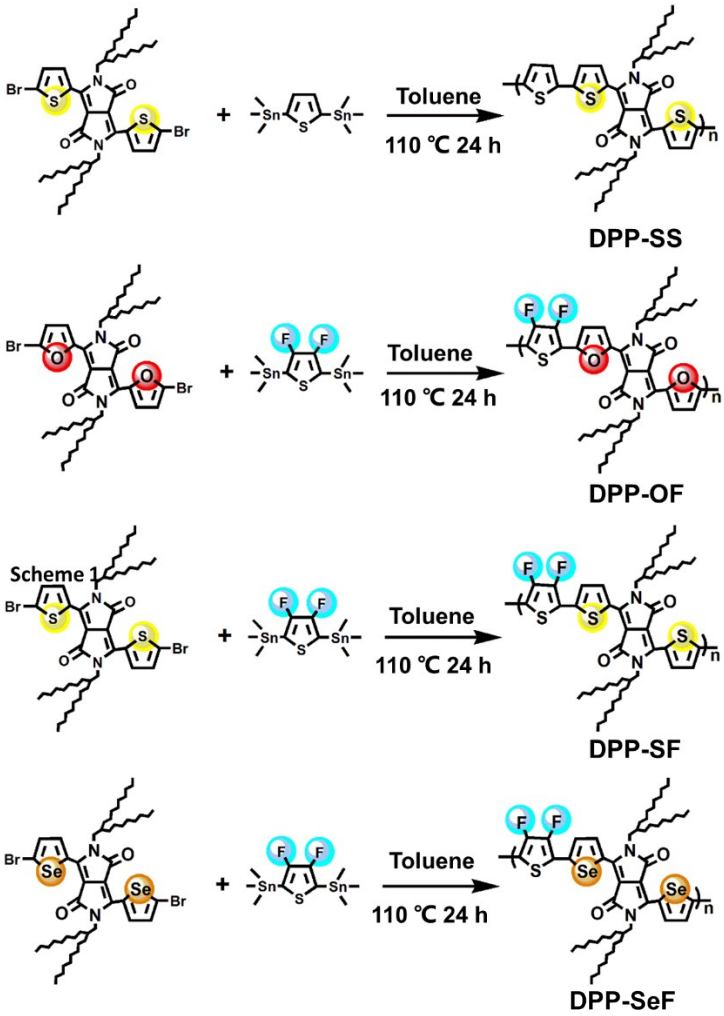

Scheme 1. Synthesis and molecular structure of DPP-SS, DPP-OF, DPP-SF and DPP-SeF NPs.

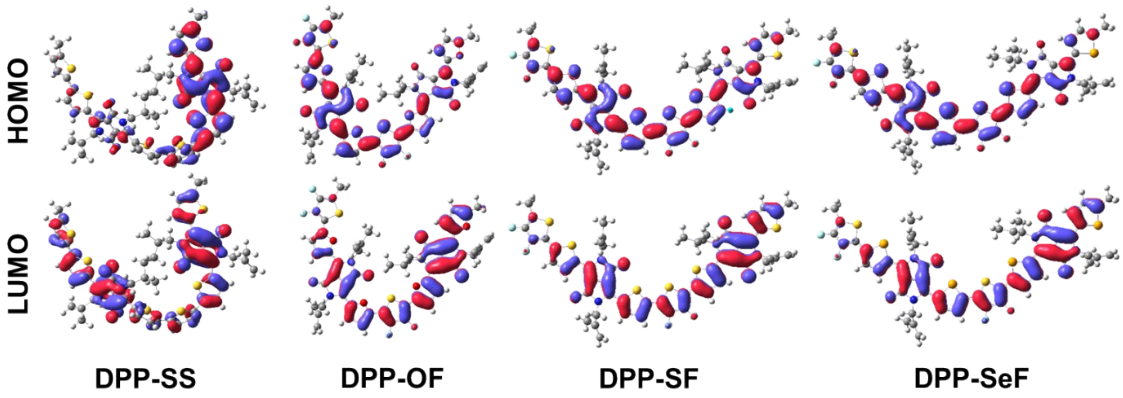

Fig. S1 The distribution of electron clouds in different energy level orbits.

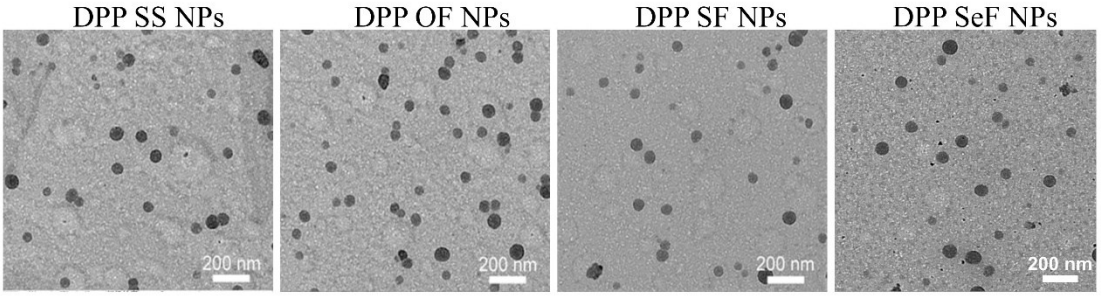

Fig. S2 The representative TEM images of DPPs NPs. Scale bar = 200 nm.

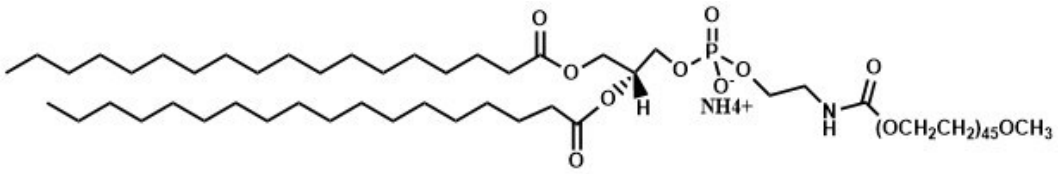

Fig. S3 Chemical structures of DSPE-mPEG$_{2000}$.

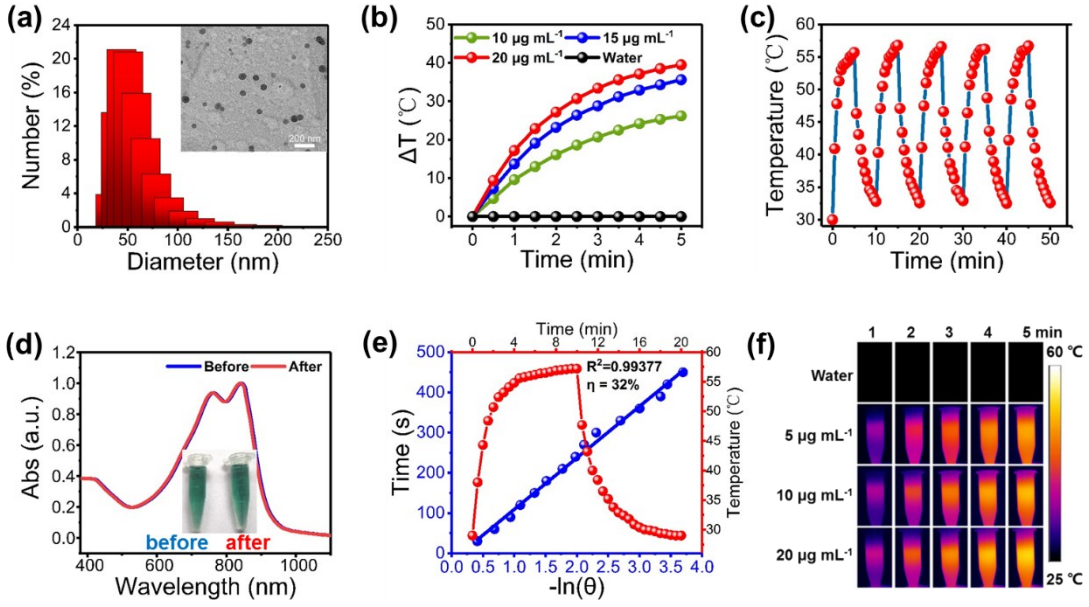

Fig. S4 (a) Representative DLS result and TEM images of DPP-SS NPs. Polydispersity index (PDI) = 0.124. (b) Temperature change curves of DPP-SS NPs with different concentrations upon exposure to 808 nm laser (0.75 W cm^{-2}, 5 min). (c) Temperature elevation of DPP-SS NPs (10.0 μg mL^{-1}) over five laser on/off cycles of 808 nm irradiation (0.75 W cm^{-2}, 10 min). (d) UV-vis spectra and solution appearance of DPP-SS NPs before and after laser irradiation. (e) Temperature change of DPP-SS NPs aqueous solution after 10 min illumination of 808 nm laser (0.75 W cm^{-2}) by naturally cooling and a

plot of time against temperature during the cooling period. (f) Thermal image of DPP-SS NPs with different concentrations upon exposure to 808 nm laser (0.75 W cm^{-2}, 5 min).

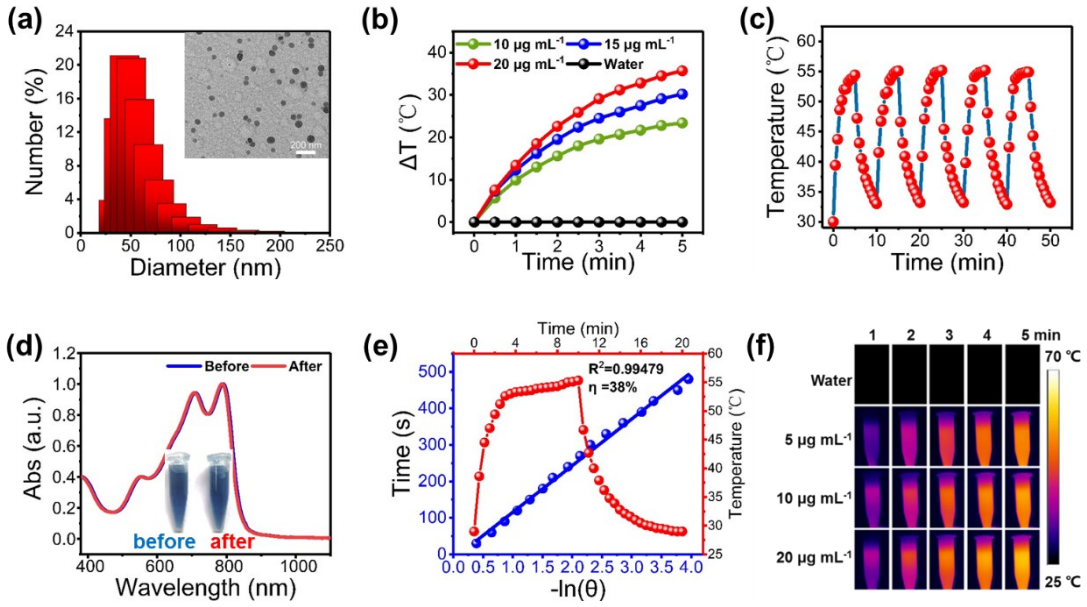

Fig. S5 (a) Representative DLS result and TEM images of DPP-OF NPs. PDI = 0.138. (b) Temperature change curves of DPP-OF NPs with different concentrations upon exposure to 808 nm laser (0.75 W cm^{-2}, 5 min). (c) Temperature elevation of DPP-OF NPs (10.0 μg mL^{-1}) over five laser on/off cycles of 808 nm irradiation (0.75 W cm^{-2}, 10 min). (d) UV-vis spectra and solution appearance of DPP-OF NPs before and after laser irradiation. (e) Temperature change of DPP-OF NPs aqueous solution after 10 min illumination of 808 nm laser (0.75 W cm^{-2}) by naturally cooling and a plot of time against temperature during the cooling period. (f) Thermal image of DPP-OF NPs with different concentrations upon exposure to 808 nm laser (0.75 W cm^{-2}, 5 min).

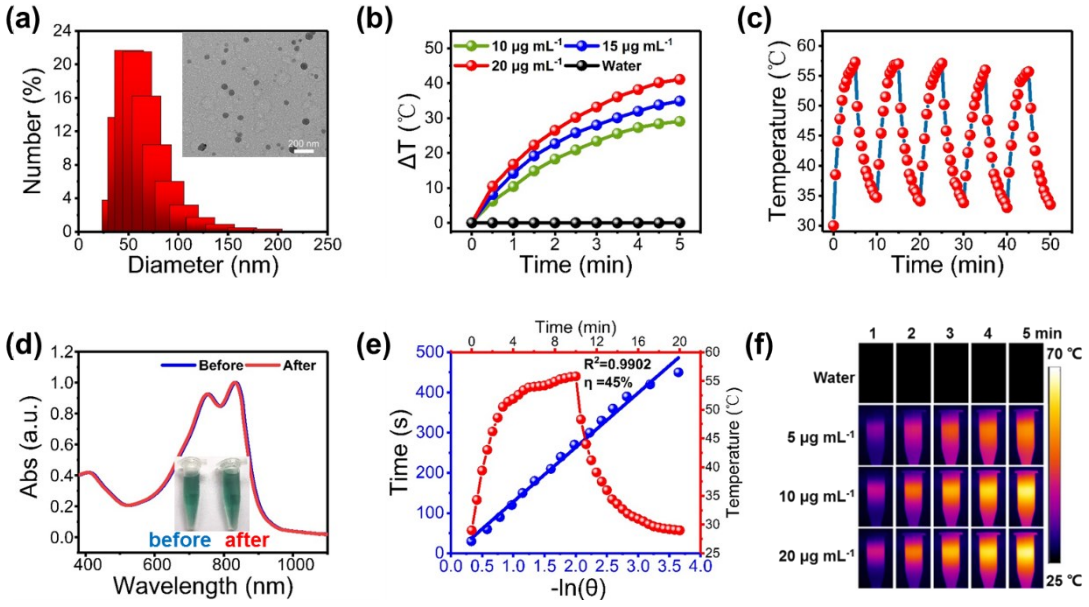

Fig. S6 (a) Representative DLS result and TEM images of DPP-SF NPs. PDI = 0.127. (b) Temperature change curves of DPP-SF NPs with different concentrations upon exposure to 808 nm laser (0.75 W cm^{-2}, 5 min). (c) Temperature elevation of DPP-SF NPs (10.0 μg mL^{-1}) over five laser on/off cycles of 808 nm irradiation (0.75 W cm^{-2}, 10 min). (d) UV-vis spectra and solution appearance of DPP-SF NPs before and after laser irradiation. (e) Temperature change of DPP-SF NPs aqueous solution after 10 min illumination of 808 nm laser (0.75 W cm^{-2}) by naturally cooling and a plot of time against temperature during the cooling period. (f) Thermal image of DPP-SF NPs with different concentrations upon exposure to 808 nm laser (0.75 W cm^{-2}, 5 min).

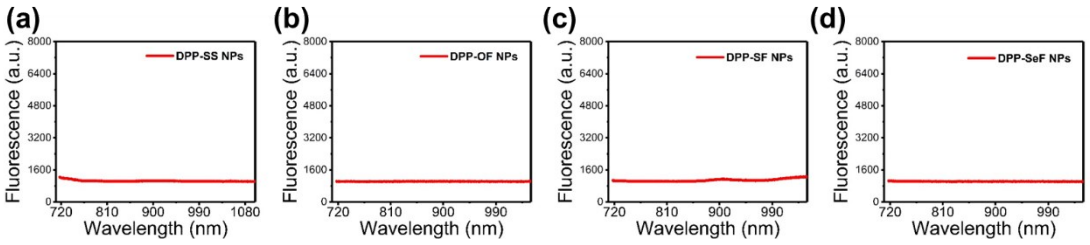

Fig. S7 Fluorescence spectrum of DPP-SS, DPP-OF, DPP-SF and DPP-SeF NPs.

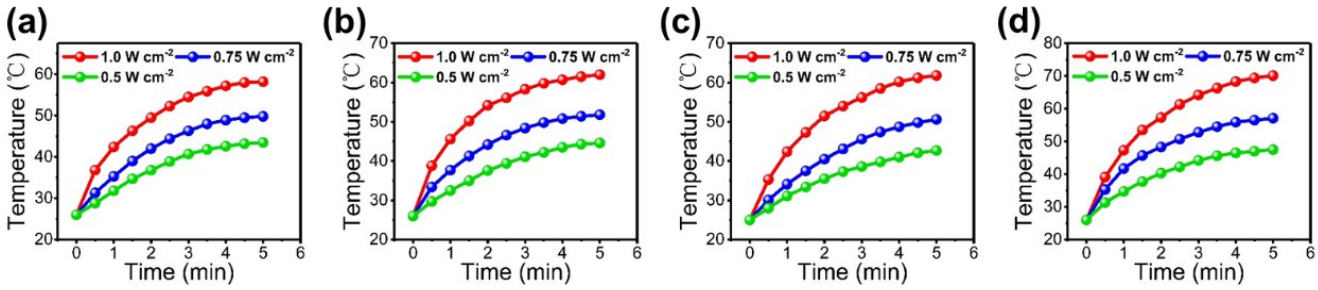

Fig. S8 Temperature change curves of NPs in different laser power: (a) DPP-SS, (b) DPP-OF, (c) DPP-SF and (d) DPP-SeF NPs (10 μg mL^{-1}).

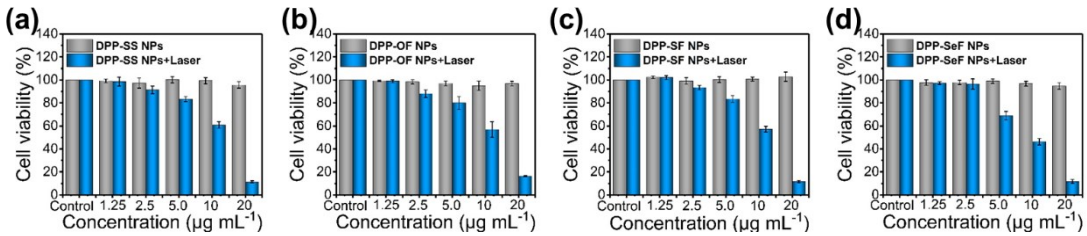

Fig. S9 Relative viabilities of H446 cells after treatment with different concentrations(0-20 μg mL^{-1}) of DPP-SeF NPs plus 808 nm laser irradiation (0.75 W cm^{-2}, 5 min).

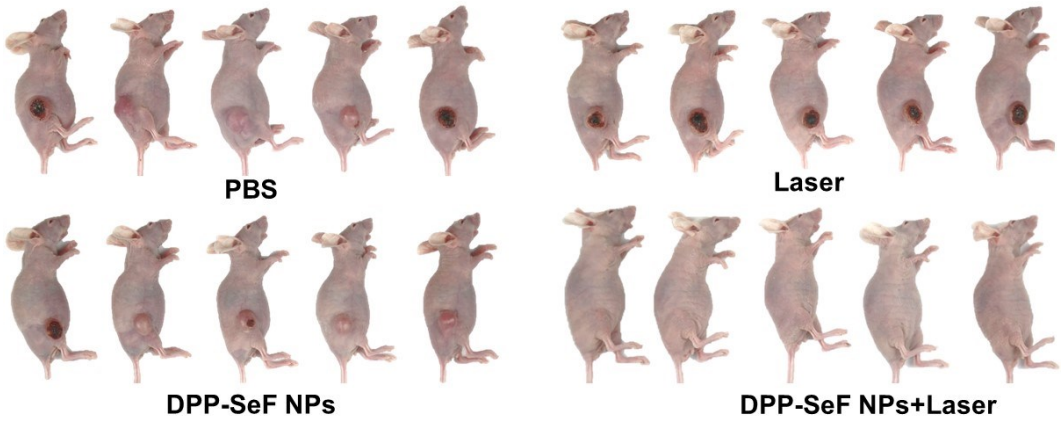

Fig. S10 Representative photographs of various post-treatment mouse after 14 days treatment.

References

(1) B. Delley, *J. Chem. Phys.* 2000, **113**, 7756.

(2) B. Delley, *J. Chem. Phys.* 1990, **92**, 508.

(3) A. D. Becke, *J. Chem. Phys.* 1988, **88**, 2547.

(4) J. P. Perdew, Y. Wang, *Phys. Rev. B,* 1992, **45**, 13244.